

Enhancement of spectral resolution and accuracy in asynchronous-optical-sampling terahertz time-domain spectroscopy for low-pressure gas-phase analysis

Takeshi Yasui,^{1,2,*} Kohji Kawamoto,¹ Yi-Da Hsieh,¹ Yoshiyuki Sakaguchi,¹ Mukesh Jewariya,² Hajime Inaba,³ Kaoru Minoshima,³ Francis Hindle,⁴ and Tsutomu Araki¹

¹Graduate School of Engineering Science, Osaka University, 1-3 Machikaneyama, Toyonaka, Osaka 560-8531, Japan

²Institute of Technology and Science, The University of Tokushima, 2-1 Minami-Josanjima, Tokushima, Tokushima 770-8506, Japan

³National Metrology Institute of Japan, National Institute of Advanced Industrial Science and Technology, 1-1-1 Umezono, Tsukuba, Ibaraki 305-8563, Japan

⁴Laboratoire de Physico-Chimie de l'Atmosphère, Université du Littoral Côte d'Opale, 189A Av. Maurice Schumann, Dunkerque 59140, France
*yasui@me.tokushima-u.ac.jp

Abstract: The spectral resolution and accuracy of asynchronous-optical-sampling terahertz time-domain spectroscopy (ASOPS-THz-TDS) were evaluated by examining low-pressure gas-phase samples. Use of dual 56-MHz, erbium (Er)-doped, mode-locked femtosecond fiber lasers enhanced the spectral resolution to as low as 50.5 MHz and the spectral accuracy to as low as 6.2×10^{-6} . The results indicate that ASOPS-THz-TDS has the potential to achieve high spectral resolution, high spectral accuracy, and wide spectral coverage at the same time. ASOPS-THz-TDS will open a new door to gas-phase spectroscopy of multiple chemical species in the field of atmospheric gas analysis.

©2012 Optical Society of America

OCIS codes: (120.6200) Spectrometers and spectroscopic instrumentation; (300.6320) Spectroscopy, high-resolution; (300.6495) Spectroscopy, terahertz.

References and links

1. M. Exter, Ch. Fattinger, and D. Grischkowsky, "Terahertz time-domain spectroscopy of water vapor," *Opt. Lett.* **14**(20), 1128–1130 (1989).
2. D. M. Mittleman, R. H. Jacobsen, R. Neelamani, R. G. Baraniuk, and M. C. Nuss, "Gas sensing using terahertz time-domain spectroscopy," *Appl. Phys. B* **67**(3), 379–390 (1998).
3. A. S. Pine, R. D. Suenram, E. R. Brown, and K. A. McIntosh, "A terahertz photomixing spectrometer: application to SO₂ self broadening," *J. Mol. Spectrosc.* **175**(1), 37–47 (1996).
4. S. Matsuura, M. Tani, H. Abe, K. Sakai, H. Ozeki, and S. Saito, "High-resolution terahertz spectroscopy by a compact radiation source based on photomixing with diode lasers in a photoconductive antenna," *J. Mol. Spectrosc.* **187**(1), 97–101 (1998).
5. G. Mouret, F. Hindle, A. Cuisset, C. Yang, R. Bocquet, M. Lours, and D. Rovera, "THz photomixing synthesizer based on a fiber frequency comb," *Opt. Express* **17**(24), 22031–22040 (2009).
6. C. Janke, M. Först, M. Nagel, H. Kurz, and A. Bartels, "Asynchronous optical sampling for high-speed characterization of integrated resonant terahertz sensors," *Opt. Lett.* **30**(11), 1405–1407 (2005).
7. T. Yasui, E. Saneyoshi, and T. Araki, "Asynchronous optical sampling terahertz time-domain spectroscopy for ultrahigh spectral resolution and rapid data acquisition," *Appl. Phys. Lett.* **87**(6), 061101 (2005).
8. G. Klatt, R. Gebbs, H. Schäfer, M. Nagel, C. Janke, A. Bartels, and T. Dekorsy, "High-resolution terahertz spectrometer," *IEEE J. Sel. Top. Quantum Electron.* **17**(1), 159–168 (2011).
9. R. A. Cheville and D. Grischkowsky, "Far-infrared terahertz time-domain spectroscopy of flames," *Opt. Lett.* **20**(15), 1646–1648 (1995).
10. D. Bigourd, A. Cuisset, F. Hindle, S. Matton, E. Fertein, R. Bocquet, and G. Mouret, "Detection and quantification of multiple molecular species in mainstream cigarette smoke by continuous-wave terahertz spectroscopy," *Opt. Lett.* **31**(15), 2356–2358 (2006).
11. T. Yasui, M. Nose, A. Ihara, K. Kawamoto, S. Yokoyama, H. Inaba, K. Minoshima, and T. Araki, "Fiber-based, hybrid terahertz spectrometer using dual fiber combs," *Opt. Lett.* **35**(10), 1689–1691 (2010).

12. H. Inaba, Y. Daimon, F.-L. Hong, A. Onae, K. Minoshima, T. R. Schibli, H. Matsumoto, M. Hirano, T. Okuno, M. Onishi, and M. Nakazawa, "Long-term measurement of optical frequencies using a simple, robust and low-noise fiber based frequency comb," *Opt. Express* **14**(12), 5223–5231 (2006).
13. M. Kessler, H. Ring, R. Trambarulo, and W. Gordy, "Microwave spectra and molecular structures of methyl cyanide and methyl isocyanide," *Phys. Rev.* **79**(1), 54–56 (1950).
14. H. M. Pickett, R. L. Poynter, E. A. Cohen, M. L. Delitsky, J. C. Pearson, and H. S. P. Muller, "Submillimeter, millimeter, and microwave spectral line catalog," *J. Quant. Spectrosc. Radiat. Transf.* **60**(5), 883–890 (1998).
15. L. S. Rothman, I. Gordon, A. Barbe, D. Benner, P. Bernath, M. Birk, V. Boudon, L. Brown, A. Campargue, J.-P. Champion, K. Chance, L. Coudert, V. Dana, V. Devi, S. Fally, J.-M. Flaud, R. Gamache, A. Goldman, D. Jacquemart, I. Kleiner, N. Lacome, W. Lafferty, J.-Y. Mandin, S. Massie, S. Mikhailenko, C. Miller, N. Moazzen-Ahmadi, O. Naumenko, A. Nikitin, J. Orphal, V. Perevalov, A. Perrin, A. Predoi-Cross, C. P. Rinsland, M. Rotger, M. Šimečková, M. A. H. Smith, K. Sung, S. A. Tashkun, J. Tennyson, R. A. Toth, A. C. Vandaele, and J. Vander Auwera, "The HITRAN 2008 molecular spectroscopic database," *J. Quant. Spectrosc. Radiat. Transf.* **110**(9-10), 533–572 (2009).
16. A. Bartels, R. Cerna, C. Kistner, A. Thoma, F. Hudert, C. Janke, and T. Dekorsy, "Ultrafast time-domain spectroscopy based on high-speed asynchronous optical sampling," *Rev. Sci. Instrum.* **78**(3), 035107 (2007).

1. Introduction

Recently, terahertz (THz) spectroscopy has emerged as a new mode for sensing and material characterization. One interesting application of THz spectroscopy is in the analysis of atmospheric molecular gases, because their rotational transitions give them particularly rich spectral fingerprints in the THz region. Measuring these densely distributed absorption lines correctly in THz spectroscopy requires high spectral resolution, high spectral accuracy, and broad spectral coverage. THz time-domain spectroscopy (THz-TDS) with pulsed THz radiation is a popular spectroscopic technique for obtaining a broadband THz spectrum [1, 2]. In this method, the frequency scale of the THz spectrum is established by mechanical time-delay scanning with a motor-driven translation stage. Therefore, the spectral resolution is determined by the reciprocal of the time window of the observed THz temporal waveform, whereas the spectral accuracy depends on the positioning precision of the translation stage used for time-delay scanning. However, limited stroke length and poor positioning precision of usual stepping-motor-driven translation stages are barriers to achieving high spectral resolution and accuracy in this method. Although the positioning accuracy can be improved largely by monitoring the stage translation with interferometer, it is still difficult to extend the stroke length largely due to the spot size variation of the laser light and/or the issue of a trade-off between the scanning range and scanning rate. On the other hand, THz spectroscopy with a tunable, narrow-linewidth, continuous-wave THz wave, namely CW-THz spectroscopy, is a promising spectroscopic technique for achieving high spectral resolution [3, 4]. However, the accuracy of the frequency scale in this method depends on the performance of an optical wavemeter employed for measuring the wavelengths of two CW near-infrared lasers used for photomixing. Although the spectral accuracy can be improved by phase-locking the two CW lasers to a single optical frequency comb [5], the spectral range of continuous tuning covered in this method is usually narrower than that in THz-TDS.

One potential method to simultaneously achieve high spectral resolution, high spectral accuracy, and broad spectral coverage in THz spectroscopy is asynchronous-optical-sampling THz-TDS (ASOPS-THz-TDS) using two mode-locked lasers with slightly mismatched mode-locked frequencies (mode-locked frequency = f_1 and f_2 , offset frequency = $\Delta f = f_2 - f_1$) for generation and detection of the pulsed THz radiation [6, 7]. Since ASOPS-THz-TDS helps to realize a time delay much longer than that achievable with a motor-driven translation stage in conventional THz-TDS, it has the potential to achieve high spectral resolution with broad spectral coverage. For example, when the measurement time window of the pulsed THz radiation is extended to one pulse period, the spectral resolution can be enhanced to the mode-locked frequency f_1 . In this case, the frequency scale of the spectrum is determined on the basis of the measurement time scale and a temporal magnification factor of $f_1/\Delta f$ [7]. However, the actual stability of f_1 and Δf may cause fluctuations in the temporal magnification factor, and hence influence the spectral resolution and accuracy. Although f_1 and/or Δf can be stabilized by referencing to a reference signal synthesized from a microwave frequency standard, the residual fluctuation will ultimately limit the performance of this

technique. Therefore, the actual spectral resolution and accuracy achieved by ASOPS-THz-TDS should be evaluated using a standard material, for example, the absorption lines of a molecular gas with a narrow linewidth. Spectral resolution and accuracy in an ASOPS-THz-TDS system equipped with Δf -stabilized, dual 1-GHz Ti:Sapphire lasers ($f_1 = 1,000,000,000$ Hz, $f_2 = 1,000,002,000$ Hz, and $\Delta f = 2$ kHz) were evaluated using molecular gasses at atmospheric pressure, resulting in the resolution of 1 GHz and accuracy of 5.7×10^5 [8]. Further enhanced performance will be required to increase the ability to identify spectral fingerprints and expand the selectivity of target gas molecules, for example, analysis of multiple chemical species in gas-phase spectroscopy under low pressure [9, 10]. In the work reported in this paper, we enhanced the spectral resolution and accuracy in ASOPS-THz-TDS by use of dual 56-MHz, f_1 - f_2 - Δf -stabilized, erbium (Er)-doped, mode-locked fiber lasers [11].

2. Experimental setup

Figure 1 shows a schematic diagram of the experimental setup in our fiber-laser-based ASOPS-THz-TDS system. A pair of self-starting, stretched-pulse, mode-locked, Er-doped fiber lasers ($\lambda_c = 1550$ nm, $\Delta t = 50$ fs, $P_{AVG} = 110$ mW, $f_1 \approx f_2 \approx 56.1$ MHz) [12] was used to generate and detect the pulsed THz radiation. The 20th-harmonic components of the mode-locked frequency ($20f_1$ and $20f_2$) were extracted from two signals detected with two fast photodetectors (PDs, bandwidth = 1.2 GHz) through electronic heterodyned processes that employ two frequency synthesizers (FS1, output freq. = $f_{FS1} = 1,112,480,000$ Hz; FS2, output freq. = $f_{FS2} = 1,112,480,100$ Hz) phase-locked to a rubidium frequency standard (Rb-FS, accuracy = 5×10^{-11} and instability = 2×10^{-11} at 1 s), two double-balanced mixers (DBMs), and two low-pass filters (LPFs). The resulting beat signals (freq. = $20f_1 - f_{FS1}$ and $20f_2 - f_{FS2}$) were used to generate the final error signals (freq. = $20f_1 - f_{FS1} - f_{Rb}$ and $20f_2 - f_{FS2} - f_{Rb}$) by mixing with output signals from Rb-FS (output freq. = $f_{Rb} = 10$ MHz). Finally, based on these error signal, the cavity length in fiber lasers was adjusted with piezoelectric actuators (quick, fine, and narrow control) and Peltier heaters (slow, coarse, and wide control) through proportional and integral control systems (PIs) so that $20f_1 - f_{FS1} - f_{Rb} = 0$ and $20f_2 - f_{FS2} - f_{Rb} = 0$, or $20f_1 = f_{FS1} + f_{Rb}$ and $20f_2 = f_{FS2} + f_{Rb}$. In this way, the individual mode-locked frequencies of the two lasers ($f_1 = 56,124,000$ Hz and $f_2 = 56,124,005$ Hz), and thus the frequency offset between them ($\Delta f = f_2 - f_1 = 5$ Hz), were stabilized by two independent laser control systems. After wavelength conversion of the two laser beams with second-harmonic-generation crystals (SHGs), pulsed THz radiation was emitted by a dipole-shaped, low-temperature-grown, GaAs photoconductive antenna triggered by pump light (PCA1), and was then detected by another dipole-shaped LT-GaAs-PCA triggered by probe light (PCA2). Portions of the output light from the two lasers were fed into a sum-frequency-generation cross-correlator (SFG-XC). The resulting SFG signal was used to generate a time origin signal in the ASOPS-THz-TDS. The temporal waveform of the pulsed THz radiation was measured with a digitizer (sampling frequency = 500 kHz) by using the SFG-XC signal as a trigger signal after amplification with a current preamplifier (AMP, bandwidth = 100 kHz, gain = 5×10^7 V/A). The time window of the measured temporal waveform was set equal to one pulse period in order to achieve a spectral resolution equal to the mode-locked frequency. To avoid pressure broadening of absorption lines, molecular gasses were enclosed in a low-pressure gas cell (length = 380 mm, diameter = 17 mm) with a pair of Brewster windows made of polypropylene plates. The optical path in which the THz beam propagated, except for the gas cell, was purged with dry nitrogen gas to avoid absorption by atmospheric moisture. Finally, the absorption spectrum was obtained by using a zero-filling factor of 10, fast Fourier transformation, and normalization with a reference spectrum obtained under identical conditions.

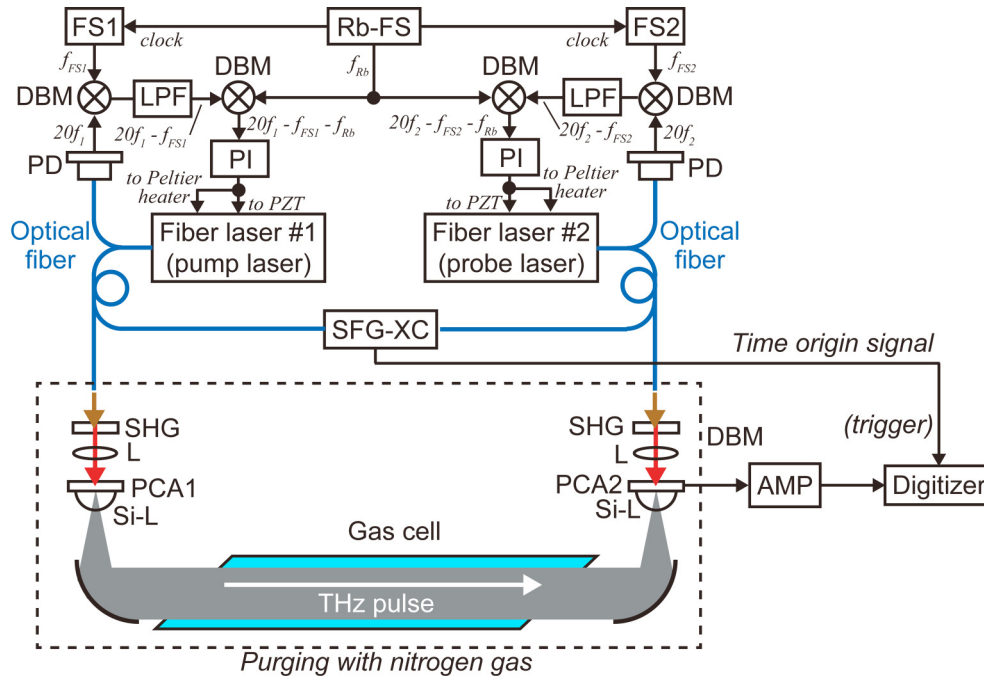


Fig. 1. Experimental setup. FS1 and FS2, frequency synthesizers; Rb-FS, rubidium frequency standard; DBMs, double-balanced mixers; LPFs, low-pass filters; PD, photodetectors; PIs, proportional and integral control systems; SFG-XC, sum-frequency-generation cross-correlator; SHGs, second-harmonic-generation crystals; Ls, lenses; PCA1, photoconductive antenna for THz generation; PCA2, photoconductive antenna for THz detector; Si-Ls, silicon lenses; AMP, current preamplifier.

3. Results

3.1 Evaluation of spectral resolution using low-pressure water vapor

To evaluate the spectral resolution, we measured the absorption spectrum of the rotational transition $1_{10} \leftarrow 1_{01}$ at 0.557 THz in water vapor. To decrease the strong absorption of water vapor, we diluted the water vapor with a foreign gas (dry argon gas). Figure 2(a) shows the absorption spectrum of the 0.557 THz water line at a total pressure of 1 kPa. In usual, signal integration of numerous scans is required in ASOPS-THz-TDS due to the fact that a lock-in amplifier cannot be used. In the present system, signal averaging of 5,000-sweep sequences under the low scan rate ($= \Delta f = 5\text{Hz}$) resulted in the required time of 1,000 s. If the scan rate is increased by use of a fast current preamplifier or free-space electro-optic sampling equipped with a fast photodetector, the data acquisition time will be decreased. The spectral linewidth was determined to be 50.5 MHz when a Lorentzian function was fitted to the spectral shape, indicated by the solid line in Fig. 2(a), which was reasonably consistent with the mode-locked frequency of 56.1 MHz. The reason for the negative absorption coefficient is mainly due to the system instability of THz spectral amplitude in the acquisition time.

Next, we investigated pressure broadening of the same water line when the total pressure was increased. Figure 2(b) shows the half-width at half-maximum (HWHM) of the observed absorption line as a function of the total pressure, which was varied between 1 kPa and 50 kPa. The linear relationship without saturation indicated that the slope gives the pressure broadening parameter of this mixed gas sample without any influence of the instrumentation linewidth or the Doppler linewidth. We determined the broadening parameter to be 31.7 MHz/kPa ($= 3.17\text{ MHz/mbar}$) with a fitting error R of 0.99955, by performing a linear approximation to $y = \alpha x$, indicated by the solid line in Fig. 2(b), where y is the HWHM, α is

the pressure broadening parameter, and x is the total pressure. Considering the obtained parameter, the self-broadening coefficient of water ($= 13.8$ MHz/mbar), the collision-broadening coefficient of argon ($= 1.63$ MHz/mbar), and the total pressure, the mixture ratio of water vapor to the argon gas was estimated to 10.4% in this experiment. From these experiments, we can conclude that our ASOPS-THz-TDS system has the potential to perform a spectral resolution comparable to the mode-locked frequency in low-pressure gas-phase spectroscopy.

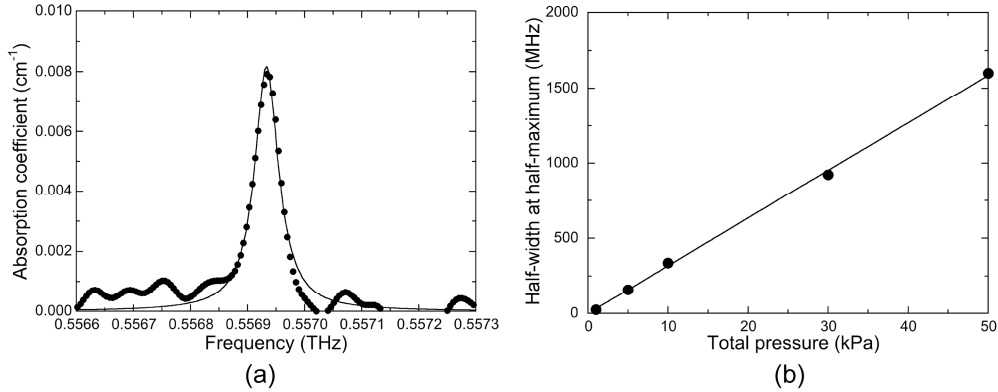


Fig. 2. (a) Water absorption spectrum of rotational transition $1_{10}-1_{01}$ at 0.557 THz (total pressure = 1 kPa) and (b) pressure broadening of 0.557 THz water line as a function of total pressure.

3.2 Evaluation of spectral accuracy using low-pressure acetonitrile gas

To evaluate the spectral accuracy and demonstrate the capacity to simultaneously probe multiple absorption lines, we performed gas-phase spectroscopy of acetonitrile (CH_3CN). As CH_3CN is a symmetric top molecule, the frequencies of absorption lines caused by its rotational transition are given by

$$\nu = 2B(J+1) - 2D_{JK}K^2(J+1) \quad (1)$$

where B is the rotational constant, J and K are rotational quantum numbers, and D_{JK} is the centrifugal distortion constant. Since CH_3CN has a B value of 9.2 GHz [13], a manifold of rotational transitions regularly spaced by $2B$ ($= 18.4$ GHz) is expected from the first term in Eq. (1). Furthermore, from the second term in Eq. (1), each absorption line composing the manifold has hyperfine structure determined by D_{JK} . Conventionally, the manifold of the rotational transitions and the hyperfine structure have been separately measured by using broadband THz-TDS [2] and a high-resolution CW-THz spectrometer [4]. Here, on the other hand, we evaluated the possibility that the ASOPS-THz-TDS system allows us to observe both features solely due to wide dynamic range of the frequency scale.

Figure 3(a) shows an amplitude spectrum of pulsed THz radiation after passing through a gas cell filled with CH_3CN at 40 Pa, in which the manifold of the regularly spaced rotational transitions was clearly found within a frequency range from 0.3 to 0.9 THz in Fig. 3(a). To observe the detailed structure of the manifold, we calculated the absorption spectrum around 0.65 THz, as shown in Fig. 3(b). The six observed absorption lines had a mutual frequency spacing of 18.4 GHz, in good agreement with the value reported in the literature [2]. We expanded the range to observe hyperfine structure of the $J = 35$ to $J = 34$ transition around 0.64 THz and assigned lines $K = 3$ to 10, as shown in Fig. 3(c). To determine the center frequencies of these absorption lines, we performed multi-peak fitting analysis using a Lorentzian function, indicated by the black solid line in Fig. 3(c). Table 1 summarizes the results for the absorption lines, showing a comparison between experimental values and values reported in JPL database [14], and the frequency discrepancy between them. The mean

and standard deviation of the discrepancy for the eight assigned absorption lines were 4 MHz and 3 MHz, respectively. When spectral accuracy is defined as the ratio of the frequency discrepancy to the value reported in the literature, the mean spectral accuracy was 6.2×10^{-6} in this experiment.

Accuracy of the absorption strength is also important to make the reliable quantitative analysis in gas-phase spectroscopy under low pressure. To evaluate the quality of the obtained spectrum, one should compare the obtained spectrum with that calculated from spectral database. However, HITRAN database is not possible as this database presently only has CH_3CN at wavenumbers from 890 - 946 cm^{-1} [15]. Although JPL database gives integrated intensities of each absorption line in this molecule [14], it is impossible to make the calculation of the complete spectrum, as there are no values for the broadening coefficients. Here, we made a simple comparison of our spectrum with the integrated intensities in JPL database, indicated as red lines in Fig. 3(c). The relative variation between neighboring lines is reasonably well reproduced and is limited by the signal-to-noise ratio of the measurements and the accuracy of the line strength calculations included in the database.

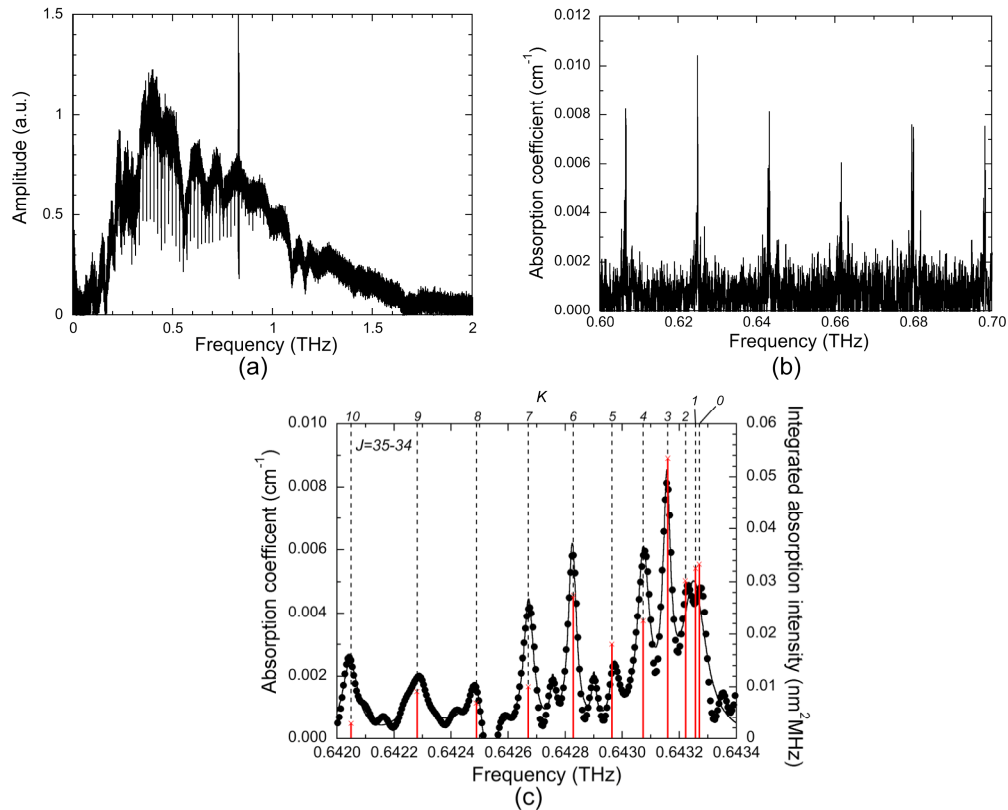


Fig. 3. (a) Amplitude spectrum of pulsed THz radiation after passing through a gas cell filled with CH_3CN at 40 Pa, (b) absorption spectrum of CH_3CN between 0.6 and 0.7 THz, and (c) expanded absorption spectrum around 0.65 THz.

Table 1. Comparison of CH₃CN absorption line positions as reported in the literature [14] and obtained using ASOPS-THz-TDS in this work.

J	K	Literature value (THz)	Experimental value (THz)	Discrepancy (MHz)
	10	0.642 049 478 7	0.642 046	4
	9	0.642 280 721 6	0.642 281	0
	8	0.642 487 872 7	0.642 483	5
	7	0.642 670 849 7	0.642 673	3
	6	0.642 829 579 3	0.642 825	5
35-34	5	0.642 963 997 8	0.642 974	10
	4	0.643 074 051 0	0.643 075	1
	3	0.643 159 694 2	0.643 156	4
	2	0.643 220 892 8	Not assigned	-
	1	0.643 257 622 0	Not assigned	-
	0	0.643 269 866 7	Not assigned	-
(Mean) ± (standard deviation)				4 ± 3

4. Discussions

We first discuss the bandwidth limitation of the present ASOPS-THz-TDS system. The spectral bandwidth observed in Fig. 3(a) was smaller than that of the previous ASOPS-THz-TDS system equipped with dual 1-GHz lasers (typically, 6 THz) [8]. We consider that the difference of spectral bandwidth between them is caused by that of the time resolution between them, rather than the pulse duration, bandwidth of the photoconductive antenna, or timing jitter between dual lasers. From the calculation of the bandwidth limitation [16] using the specifications of our system (electric bandwidth of current preamplifier = 100 kHz, $f_1 = 56,124,000$ Hz, and $\Delta f = 5$ Hz), a time resolution of the present system is estimated to be 0.89 ps. This resolution leads to the available bandwidth of 1.2 THz, which is reasonably consistent with the spectral bandwidth in Fig. 3(a). To extend the spectral bandwidth, it is required to increase electric bandwidth and/or Δf while keeping the good stability of the temporal magnification factor of $f_1/\Delta f$.

It will be also interesting to compare our f_1 - f_2 - Δf -stabilized, 56-MHz ASOPS-THz-TDS system with the previous Δf -stabilized, 1-GHz ASOPS-THz-TDS system from the viewpoint of the spectral resolution. One important factor to limit the actual resolution in ASOPS-THz-TDS is the accumulated timing jitter per time increment at the end of the sample interval [16]. This is because such the timing jitter fluctuates the size of the time-delay window and hence the spectral resolution. We estimated from the accumulated timing jitter of 300 fs [11] and the pulse period of 17.8 ns in our system that the contribution of the timing jitter to the spectral resolution was 0.9 kHz. On the other hand, the jitter contribution in the previous system was estimated to be 0.2 MHz to the spectral resolution [8]. Although the jitter contribution to the spectral resolution in our system is much smaller than that in the previous system, both contributions are negligible to the actual spectral resolution. Therefore, we can conclude that simultaneous stabilization of f_1 , f_2 , and Δf in our system does not make much sense at the present time. However, if the spectral resolution in ASOPS-THz-TDS can go down below 1 MHz, one may have to consider the jitter contribution caused by unstabilized f_1 and f_2 . Further work is in progress to enhance the spectral resolution of ASOPS-THz-TDS.

Finally, we discussed the spectral accuracy in ASOPS-THz-TDS. The accuracy in our system was 10-times better than that obtained with the previous ASOPS-THz-TDS system [8]. One reason for the improved accuracy is that the frequency resolution is greatly enhanced by use of a lower mode-locked frequency rather than simultaneous stabilization of f_1 , f_2 , and Δf as discussed above. Also, the accuracy of the temporal magnification factor ($f_1/\Delta f$) will

limit the useful accuracy to around 10^{-6} . Another factor to limit the spectral accuracy is existence of fluctuated background in the spectrum as observed in Fig. 2(a) although the background should be zero line to obtain the good fitting result to the experimental data. Fitting error caused by the fluctuated background also influences the spectral accuracy. The present results are therefore within the experimental uncertainty when compared with the tabulated values.

5. Conclusion

ASOPS-THz-TDS system, equipped with dual 56-MHz fiber lasers, achieved a spectral resolution of 50.5 MHz and a frequency accuracy of 6.2×10^{-6} over a spectral range of 0-2 THz. The achieved resolution and accuracy were respectively 20-times and 10-times better than those obtained with the previous ASOPS-THz-TDS system equipped with dual 1-GHz Ti:Sapphire lasers [8]. The results clearly indicate the superior performance of this system for gas-phase spectroscopy of multiple chemical species under low pressure. Finally, it should be emphasized that the frequency scale of THz spectrum established in our ASOPS-THz-TDS is traceable to Rb-ST within 6.2×10^{-6} by stabilizing f_i and Δf . An assured traceability of the frequency scale to the frequency standard is a big advantage of this method over conventional THz spectroscopic methods without any traceability system, and hence opens the door for establishment of frequency metrology in THz spectroscopy.

Acknowledgments

This work was supported by Collaborative Research Based on Industrial Demand from the Japan Science and Technology Agency, and Grants-in-Aid for Scientific Research 21360039 and 23656265 from the Ministry of Education, Culture, Sports, Science, and Technology of Japan. We also gratefully acknowledge financial support from the Renovation Center of Instruments for Science Education and Technology at Osaka University. We are grateful to Dr. Hiromichi Hoshina of RIKEN for fruitful discussions.